Numerical investigation of parallel and quasi-parallel slider bearings operating under ThermoElastoHydroDynamic (TEHD) regime

Anastassios Charitopoulos, Michel Fillon, Christos Papadopoulos

Numerical investigation of parallel and quasi-parallel slider bearings operating under ThermoElastoHydroDynamic (TEHD) Regime

Anastassios Charitopoulos [a,b,*], Michel Fillon [a], Christos I. Papadopoulos [b]
*anastasios.charitopoulos@univ-poitiers.fr
[a]Institut Pprime, CNRS - University of Poitiers -ISAE- ENSMA, Dpt GMSC, Futuroscope Chasseneuil, France
[b]School of Naval Architecture and Marine Engineering, NTUA, Zografos, Greece

Abstract. In the present work, a CFD numerical investigation of the tribological characteristics of parallel and quasi-parallel slider bearings has been performed. The work is initiated following experimental observations of load carrying capacity on parallel thrust bearings. The computational results conclude that the principal mechanism of pressure build-up is the hydrodynamic wedge generated due to thermal deformation of the active pad surface. The calculated final geometry of the pad consists of a converging region, extending from the oil entrance to the maximum pressure region, and a diverging region extending from the maximum pressure region to the oil outflow. Finally, initial surface defects of the pad active surface, contribute moderately to building-up the final load carrying capacity of the slider.

Keywords: Thermoelastohydrodynamic (TEHD) regime; Slider bearing; Parallel surface; Thermal deformation.

INTRODUCTION

The parallel slider exhibits an anomalous behaviour in terms of the classic lubrication theory, which states that a parallel slider cannot support the observed, by the experiments, loads [1-4]. Many different explanations have been proposed in the literature. Those can be categorised in three different groups: (a) geometrical imperfections of the pad and the runner surfaces that generate pressure build-up [4-11], (b) variations of the lubricant properties (mainly lubricant viscosity) in the film domain [12-15], and (c) distortion of the pad geometry due to thermal or mechanical deformations [16-21]. Regarding geometrical imperfections, it is well known that it is impossible to manufacture sliders or bearings with perfect parallel surfaces, or no leading-edge imperfections, thus the tolerances of what is considered as parallel surface needs to be investigated. Moreover, in experiments conducted with rough and polished parallel thrust bearings, differences of the results have been observed, but those differences were not large enough to drive to the conclusion that the small geometrical imperfections of the polished thrust bearing are the only reason of load carrying capacity of a parallel surface thrust bearing or slider [3]. On a different path, the leading-edge imperfection has been considered to account for pressure build-up, operating as a small tapered-land geometry. However, this geometry wedge is limited to a very small part of the bearing or slider, therefore offering only a small contribution to pressure build-up. The other major category of publications on the present subject is the existence of a so-called “viscosity wedge”. The variation of pressure and temperature in the fluid domain, generate a viscosity variation, leading to a wedge effect capable of generating oil pressure. Finally, other researchers [22] have suggested that the inertia forces and the fluid expansion play also a significant role in the parallel slider load carrying capacity. The last major group of publications on this phenomenon, is the thermal deformation of the pad geometry, due to temperature gradients at the bearing-oil interface. This would alter the geometry between the two initially parallel surfaces, leading to generation of a non-parallel fluid film shape. This shape is considered to be a converging wedge at the entrance of the lubricant, therefore generating the load carrying capacity of the parallel bearing or slider. This last assumption is consistent with the results of experimental observations [3], since the load carrying

capacity of such bearings is less pronounced during the start-up of the experimental procedure, however, as the experimental tests progress, the generated heat alters substantially the solid temperature values, causing thermal deformation, which leads to a rapid increase of the observed load carrying capacity.
In the present work, a CFD-based thermoelastohydrodynamic (TEHD) computational approach is used to study the tribological performance of quasi-parallel as well as parallel slider bearings. The paper is organized as follows: The problem definition and computational approach are first presented. Simulation results are then presented and discussed, and, finally, the main findings are summarized.

NUMERICAL MODEL

Problem description

In the present study, a three-dimensional CFD-based TEHD model of a slider bearing has been generated. A CFD model has been utilized for the calculation of flow, pressure build-up and heat dissipation in the fluid domain, as well as for the conjugate heat transfer through the solid parts of the bearing. A Finite Element (FE) model of the pad geometry has been used to calculate the thermal and mechanical deformations of the bearing pad. Further, a two-way Fluid Surface Interaction (FSI) approach has been used in order to transfer the interface pressure and thermal loads between the fluid and the solid solvers.

The numerical procedure of the present study comprises the following steps:

- First, the FE solver calculates the initial thermal expansion of the pad geometry, from an initial temperature of 20 ^{o}C to the ambient temperature of 40 ^{o}C, and transfers the displaced geometry to the CFD solver.
- The Navier-Stokes and the energy equations are solved in the lubricant and slider domains, respectively, calculating the corresponding flow and temperature distributions.
- The pressure and heat flux at the fluid/pad interface are transferred to the FE solver, which calculates the thermal and mechanical deformations of the pad.
- The displaced geometry of the pad is transferred to the CFD solver, and an updated lubricant geometry is computed.
- This described procedure iterates until final convergence, which is reached if the difference of the geometry change (measured in terms of maximum nodal mesh displacement between two consecutive steps) is less than $3x10^{-8}$.
- The performance indices of the bearing are calculated for the final converged film geometry.

The above procedure is followed for different values of the initial distance between the slider and the pad. The computational calculation algorithm is depicted in Fig. 1.

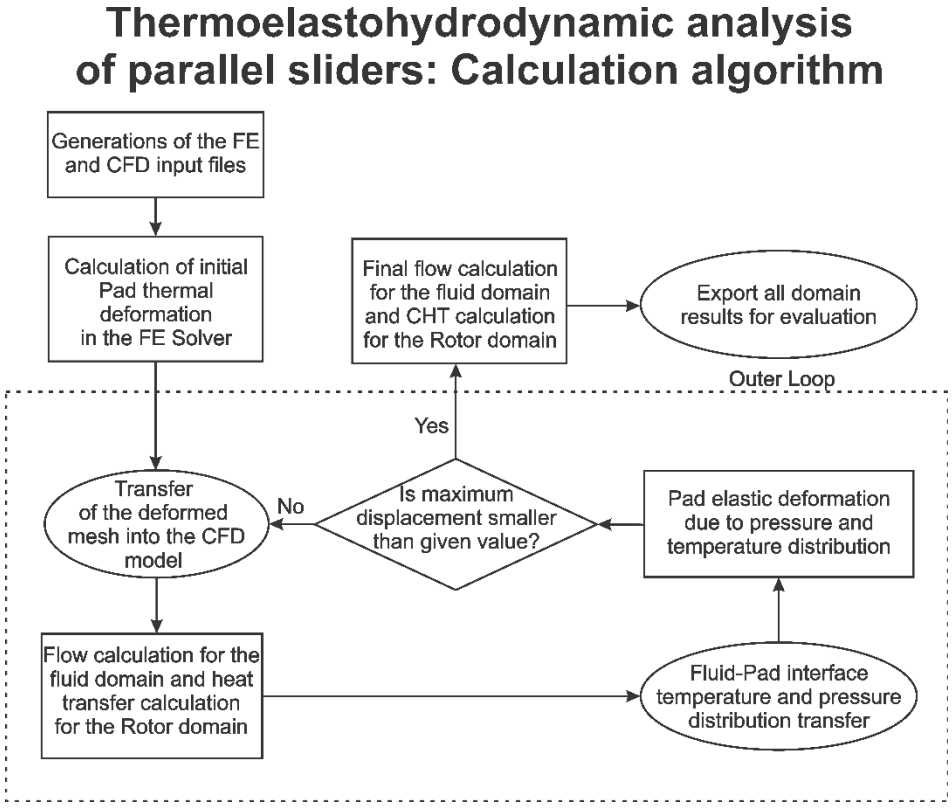

Fig. 1- Thermoelastohydrodynamic analysis of parallel slider bearings: Calculation algorithm.

In the present model, the conservation equations are solved with the CFD code ANSYS CFX and the FE code ANSYS MECHANICAL, for steady, incompressible flow, with no gravitational forces and **no cavitation** modeling. The equations are presented below:

Mass conservation equation:	$\nabla \cdot V = 0$	[1]
Momentum equations:	$\rho(V\Delta)V = -\nabla p + \nabla \cdot (\mu \cdot \nabla V)$	[2]
Energy equation, fluid domain:	$\rho \cdot c_{pf} \cdot v \cdot \nabla T = \nabla(\lambda_f \cdot \nabla T) + \mu\Phi$	[3]
Energy equation, solid domains:	$\nabla(\lambda_s \cdot \nabla T) = 0$	[4]

Where V is the velocity vector (m/s), p the static pressure (Pa), T the temperature (K), τ the viscous stress tensor, ρ the oil density (kg/m^3), μ the oil dynamic viscosity (kg/m.s), c_{pf} the oil specific heat capacity (J/kg.K), λ_f the oil thermal conductivity (W/m.K), λ_s the runner thermal conductivity (W/m.K). The dissipation term Φ describes the heat generated by internal fluid friction.

The pad undergoes elastic deformation due to (a) pressure distribution on the fluid/pad interface, and (b) the thermal expansion of the solid. The stress is related to strain by:

$$\{\sigma\}=[D][\{\varepsilon^{el}\}] \quad [5]$$

where $$\{\varepsilon^{el}\}=\{\varepsilon\}-\{\varepsilon^{th}\}, \text{ and } \{\varepsilon^{th}\}= \Delta T[\alpha^{se}\ \alpha^{se}\ \alpha^{se}\ 0\ 0\ 0]^T \quad [6]$$

where α^{se},is the coefficients of thermal expansion.

The load carrying capacity (LCC) of the slider is calculated as the integral of positive pressure over the fluid/pad interface:

$$LCC = \iint_{FSI} p(x,y)\,dx\,dy \quad [7]$$

Where:

$$p(x,y) = \begin{cases} p & p>0 \\ 0 & p<0 \end{cases} \quad [8]$$

The friction force is calculated as the integral of the shear force component over the fluid/pad interface.

$$Fr = \iint_{FSI} F_y(x,y)\,dx\,dy \quad [9]$$

Geometry

The present computational model consists of three domains: the pad, the fluid, and the runner. The geometrical dimensions and operating conditions have been selected as close as possible to those of the thrust bearing of the experiment of Henry et al. [3]. The fluid domain is defined by the space between the runner and pad, which contains the thin film region and half groove fore and half groove aft. This configuration has been selected in order to account for the oil mixing and the hot oil carry-over phenomena.

Table 1– Dimensions of the slider bearing model of the present study.

Dimension	Value	Units
Pad Length (L)	24.489	mm
Pad Width (B)	20	mm
Pad Thickness	10	mm
Runner Thickness	20	mm
Groove Length	3	mm
Groove Depth	4	mm
Defect Amplitude	1	μm

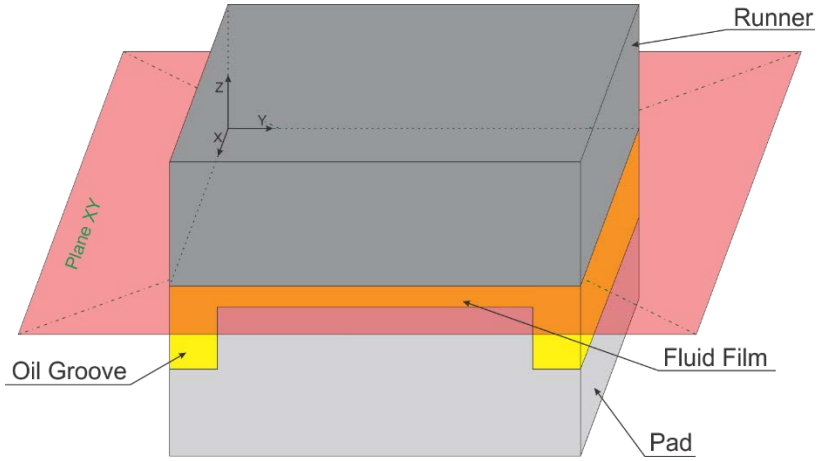

Fig. 2 - 3D representation of the solid and fluid domains of the slider bearing. Origin point.

In the present study, the fluid/pad interface has not been considered as a “perfect” parallel surface. In particular, a sinusoidal surface defect has been introduced (Fig. 3). From industrial applications, the typical specific load for such geometries is between 0.13 MPa and 0.7 MPa, but larger specific pressures can be acquired, in the order of magnitude of 1.5 MPa. The minimum film thickness of parallel thrust slider bearings operating at a specific load of approximately 1.5 MPa is of the order of few microns, as that of the typical surface defect amplitudes. Therefore, it can easily be assumed that those defects will be affecting the hydrodynamic lubrication characteristics of the parallel thrust slider bearing. In that direction, an initial surface defect was chosen for the following calculations. The reference magnitude of the defect is 1μm, as the smallest defect amplitude observed in the experimental study of Henry [3].

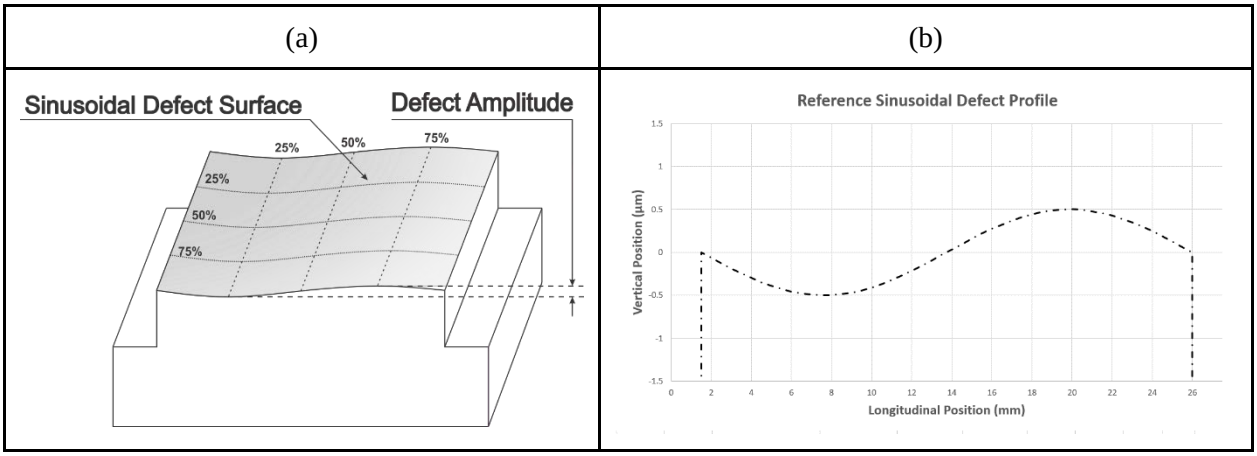

Fig. 3 - (a) Initial Pad quasi-parallel surface. (b) Plot of reference sinusoidal defect (1μm).

Boundary Conditions

The slider is consider fully flooded, with feeding pressure at the fluid inner surface, as denoted in Fig. 4. The thermal boundary conditions of the slider bearing system have been considered following the work in [23], see Fig. 4 and Table 2. The runner is considered rigid. The pad is considered fixed on the bottom surface (no displacements or rotations allowed). The thermophysical properties of the pad and runner materials are presented in Table 3. The thermophysical properties of the oil are presented in Table 4. The density of the lubrication oil utilized (ISO VG 46) is 870 kg/m3, while a temperature dependent viscosity is considered, modeled according to the McCoull and Walther relation [24]:

$$\log(\log(v+a)) = b - n\log(T)$$

where, v is the kinematic viscosity (cSt), and a = 0.6, b = 9.02865 and n = 3.52681.

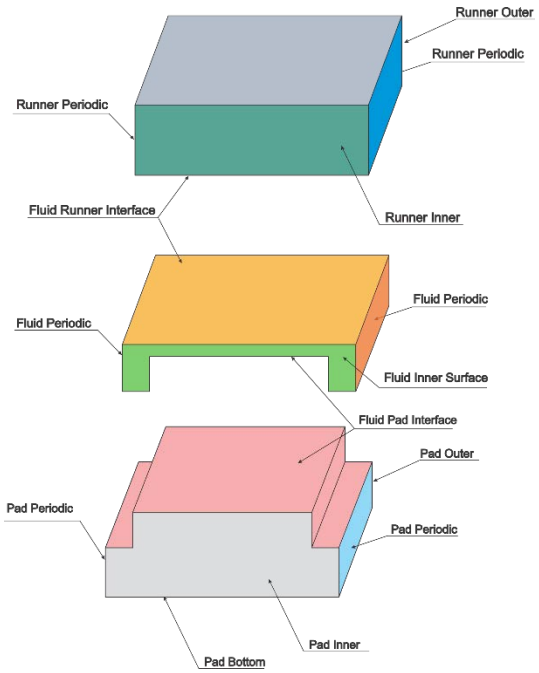

Fig. 4 - Computational model: designation domains surfaces.

Table 2 - Boundary conditions of the models.

Pad		
Top surface	Fluid-Solid interface: Continuity of heat flux and temperature	Free displacement in all directions
Bottom surface	Heat transfer coefficient: 1000 W/(m^2.K), T=40 ºC	Fixed
Inner surface	Heat transfer coefficient: 200 W/(m^2.K), T=40 ºC	Free displacement in all directions
Outer surface	Heat transfer coefficient: 25 W/(m^2.K), T=40 ºC	Free displacement in all directions
Sides	Periodic conditions	Free displacement in z and x directions
Runner		
Top surface	Heat transfer coefficient: 25 W/(m^2.K), T=20 ºC	Fixed
Bottom surface	Fluid-Solid interface: Continuity of heat flux and temperature	Fixed
Inner surface	Heat transfer coefficient: 1000 W/(m^2.K), T=20 ºC	Fixed
Outer surface	Heat transfer coefficient: 25 W/(m^2.), T=20 ºC	Fixed
Sides	Periodic conditions	Fixed
Fluid		
Fluid/Runner interface	Fluid-Solid interface: Continuity of heat flux and temperature	Fixed
Fluid/Pad interface	Fluid-Solid interface: Continuity of heat flux and temperature	Free displacement in all directions
Fluid Sides	Periodic conditions	Free displacement in z and x directions
Fluid Inner surface	Opening with temperature 40 ºC and static relative pressure 1 bar	Free displacement in z and x directions
Fluid Outer surface	Opening with temperature 20 ºC and static relative pressure 0 bar	Free displacement in z and x directions

Table 3 - Thermophysical properties of the pad and runner materials.

Property	Runner(Steel)	Pad (Copper)	Units
Specific Heat Capacity	434	377	J/(kg.K)
Thermal Conductivity	60.5	385	W/(m.K)
Molar Mass	55.85	63.55	kg/kmol
Density	7854	8933	kg/m^3
Thermal Expansion Coef.	-	$1.8x10^{-5}$	C^{-1}
Young's Modulus	-	$1.17x10^{11}$	Pa

Table 4 - Thermophysical oil properties.

ISO VG 46 Oil Parameters			
Symbol	Value	Units	Comments
ρ	870	kg m^3	Oil density
c	2.1	kJ (kg.K)	Specific heat capacity
k	0.13	W/(m.K)	Thermal conductivity

Meshing procedure

The final mesh parameters of the present model have been selected following a detailed mesh study, presented in Appendix A. Regarding the pad domain, due to the thermal and mechanical deformations, a dense hexahedral mesh has been utilised, composed of 127,310 elements. The fluid domain is discretized with hexahedral elements, utilizing 18 layers of elements in the cross-flow (film thickness) direction, whereas in the longitudinal and transverse directions, 156 and 70 elements have been used, respectively. The total number of elements in the fluid and runner domains is 268,240. The runner domain is assumed rigid, therefore, only the heat transfer equations are solved. Simple tetrahedral elements have been selected for simplifying the meshing procedure. The number of elements used for discretizing the pad geometry is approximately 600,000 elements. Mesh details about the computational domain are presented in Fig. 5.

(a)	*(b)*	*(c)*
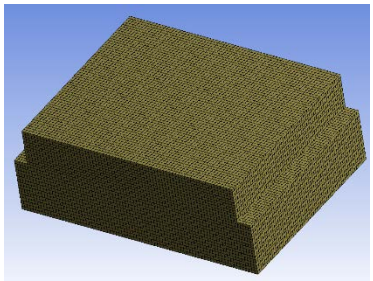	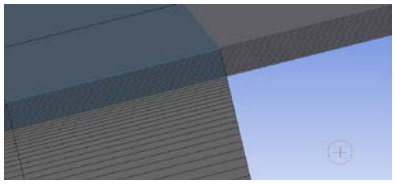	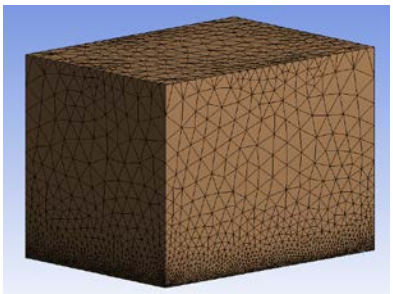

Fig. 5 - Mesh details of the computational domain: (a) Pad mesh details. (b) Fluid mesh details. (c) Runner mesh details.

THERMOELASTOHYDRODYNAMIC ANALYSIS OF BEARING OPERATION

Comparison between TEHD, THD with mechanical deformations and THD analyses

As reported in the introduction of the present work, different physical mechanisms have been proposed to explain the capability of parallel thrust bearings to support thrust load. In the present section, in order to quantify the effect of each pressure build-up mechanism, three different numerical models have been generated, with the same initial sinusoidal defect geometry (defect amplitude of 1 μm, see also Fig. 3), and their results have been assessed. In particular, (a) a TEHD model, taking into consideration the thermal and mechanical deformations of the bearing pad, (b) a THD model taking also into consideration only the mechanical deformations, assuming a very small value of thermal expansion coefficient of the bearing pad (order of magnitude $2x10^{-45}$), and (c) a THD model, assuming that the bearing pad is non-deformable, have been generated . The first model (TEHD) accounts for almost all pressure build-up mechanisms suggested in the literature, except for micro-asperity lubrication. The second model (THD with mechanical deformations) accounts for elastic deformations of the bearing pad, but neglects thermal deformations due to temperature gradients. In the third model (THD), the bearing pad and runner are assumed rigid, therefore the film geometry remains constant throughout the simulations. In all three models, a steady-state simulation scheme is selected, whereas cavitation is not taken into consideration.

The results of the three different models are presented in Fig. 6 and 7. The presented results have been acquired for constant runner velocity of 22 m/s and constant thrust load of 226 N ± 3 N. The feeding temperature is assumed to be constant and equal to 40 °C (imposed boundary condition at "Fluid Inner surface"). Large differences are observed between the calculation results of each model. In particular, maximum lubricant temperature attains a lower value for the TEHD analysis, whereas minimum film thickness and maximum pressure are substantially higher. The differences of the calculated bearing performance indices across the three different analyses vary from 5% to 30%, leading to the conclusion that the thermal deformation of the bearing pad, account only in the TEHD analysis, plays a significant role in the pressure build-up behavior of the system, affecting substantially the performance indices of the bearing.

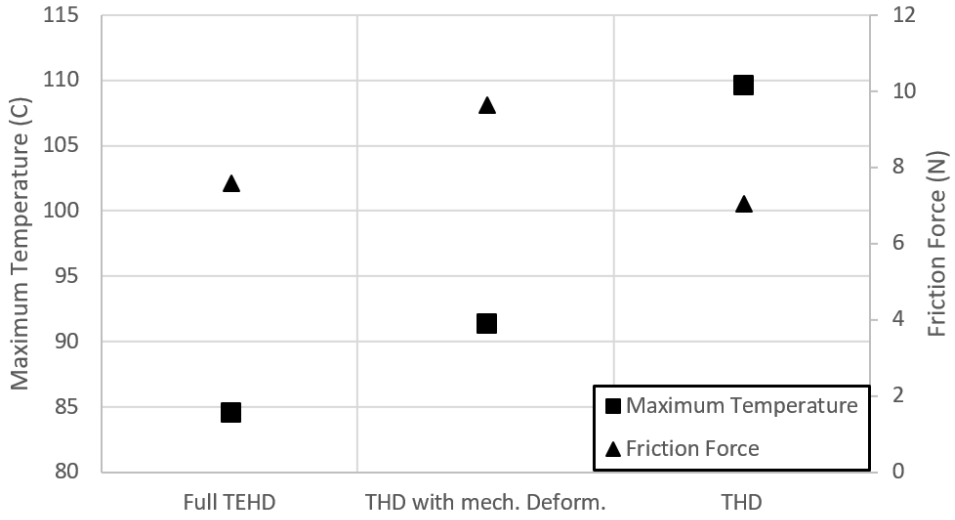

Fig. 6 – Thrust load: 226 N, Runner velocity: 22 m/s: Calculated maximum temperature at the fluid/pad interface and friction force, corresponding to (a) TEHD analysis, (b) THD with mechanical deformation analysis, and (c) THD analysis.

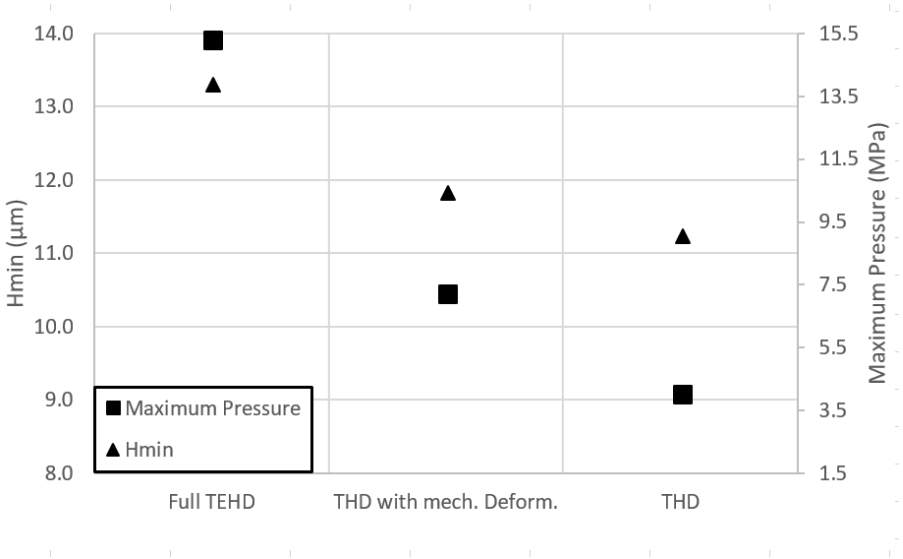

Fig. 7 – Thrust load: 226 N, Runner velocity: 22 m/s: Calculated minimum film thickness and maximum lubricant pressure, corresponding to (a) TEHD analysis, (b) THD with mechanical deformation analysis, and (c) THD analysis.

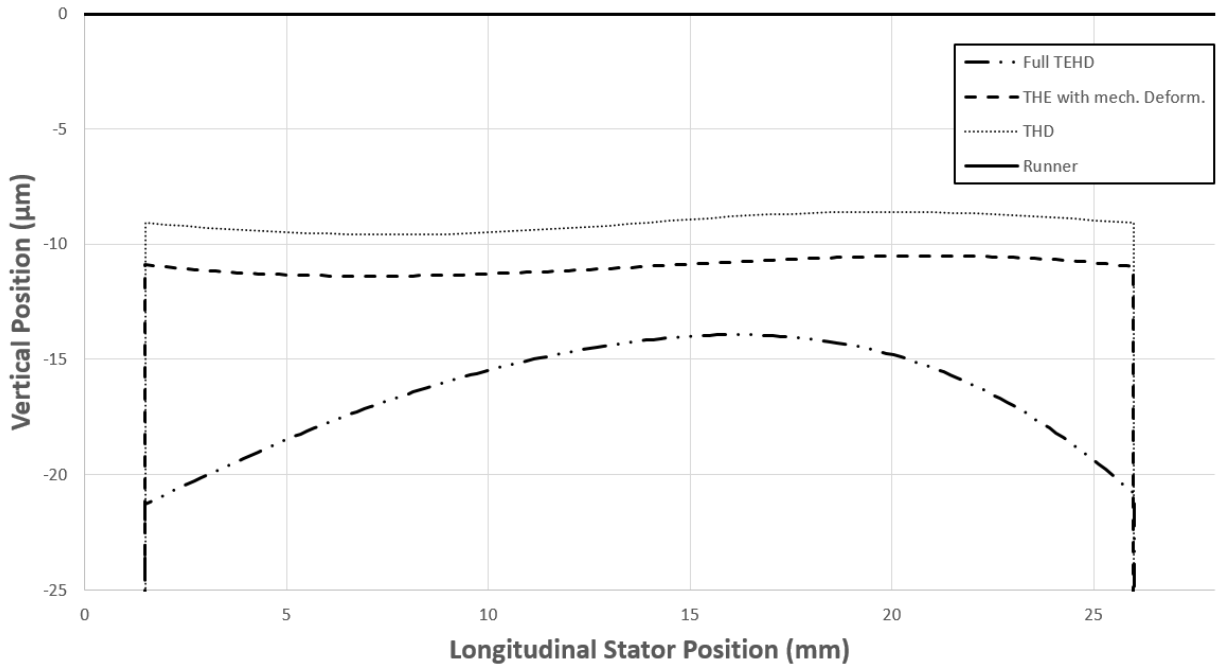

Fig. 8 - Thrust load: 226 N, Runner velocity: 22 m/s: Calculated bearing pad profiles at the longitudinal mid-section, corresponding to (a) TEHD analysis, (b) THD with mechanical deformation analysis, and (c) THD analysis.

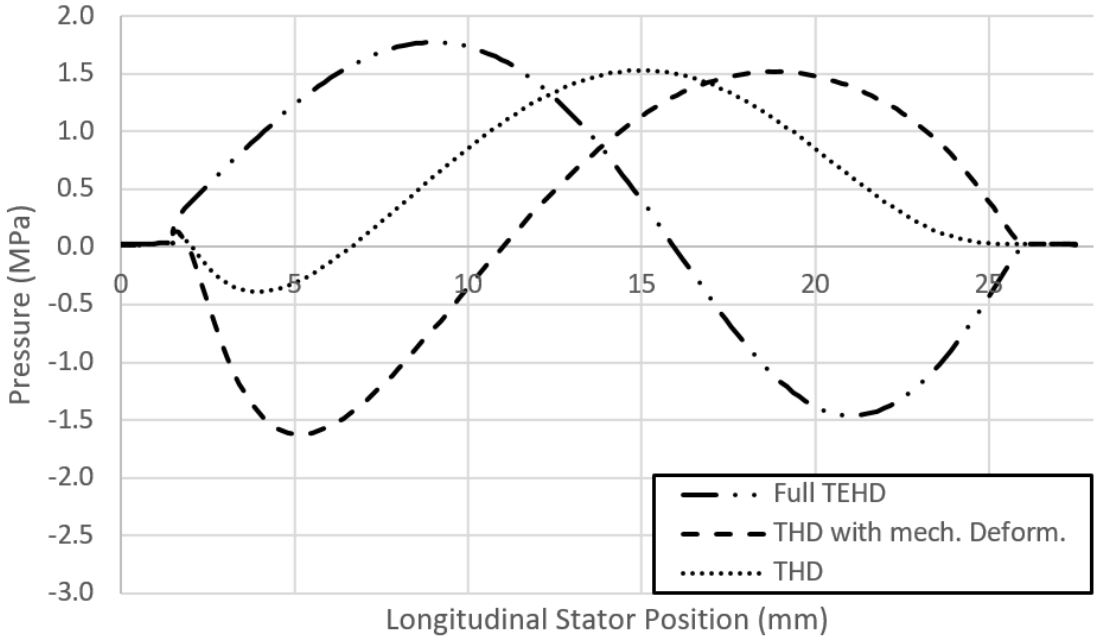

Fig. 9 – Thrust load: 226 N, Runner velocity: 22 m/s: Calculated pressure profiles along the longitudinal mid-section of the bearing pad, corresponding to (a) TEHD analysis, (b) THD with mechanical deformation analysis, and (c) THD analysis.

In Fig. 8, the three final film shapes are depicted for each of the three different analyses. The final minimum film thickness predicted by the THD model is the lowest amongst the three different models, and thus resulting to the largest values of oil temperature. The THD model with mechanical deformation (not accounting for thermal deformation) yields a bearing pad geometry in close resemblance to the initial geometry, but with small alterations which conclude to larger minimum film thickness. The pressure profiles for the three different models are depicted in the Fig. 9, and they present different regions of maximum pressure for the different modeling techniques. In the TEHD model, the high pressure region is close to the leading edge, the exact opposite of the THD with mechanical deformation. The THD model presents a maximum pressure region near the middle of the pad, with no large negative pressure region. The different behaviour of the pressure distribution on the three models is due to the final film geometry differences. Here, it should be noted that the high pressure zone was also measured in the leading edge zone of the pads by Henry et al. [3] for the configuration of the parallel surfaces thrust bearings, as it is calculated by the TEHD model. Moreover, in Fig. 10, the pressure temperature contours are depicted. The temperatures at the fluid pad interface are lower for the TEHD model, whereas those of the THD model are considerably higher.

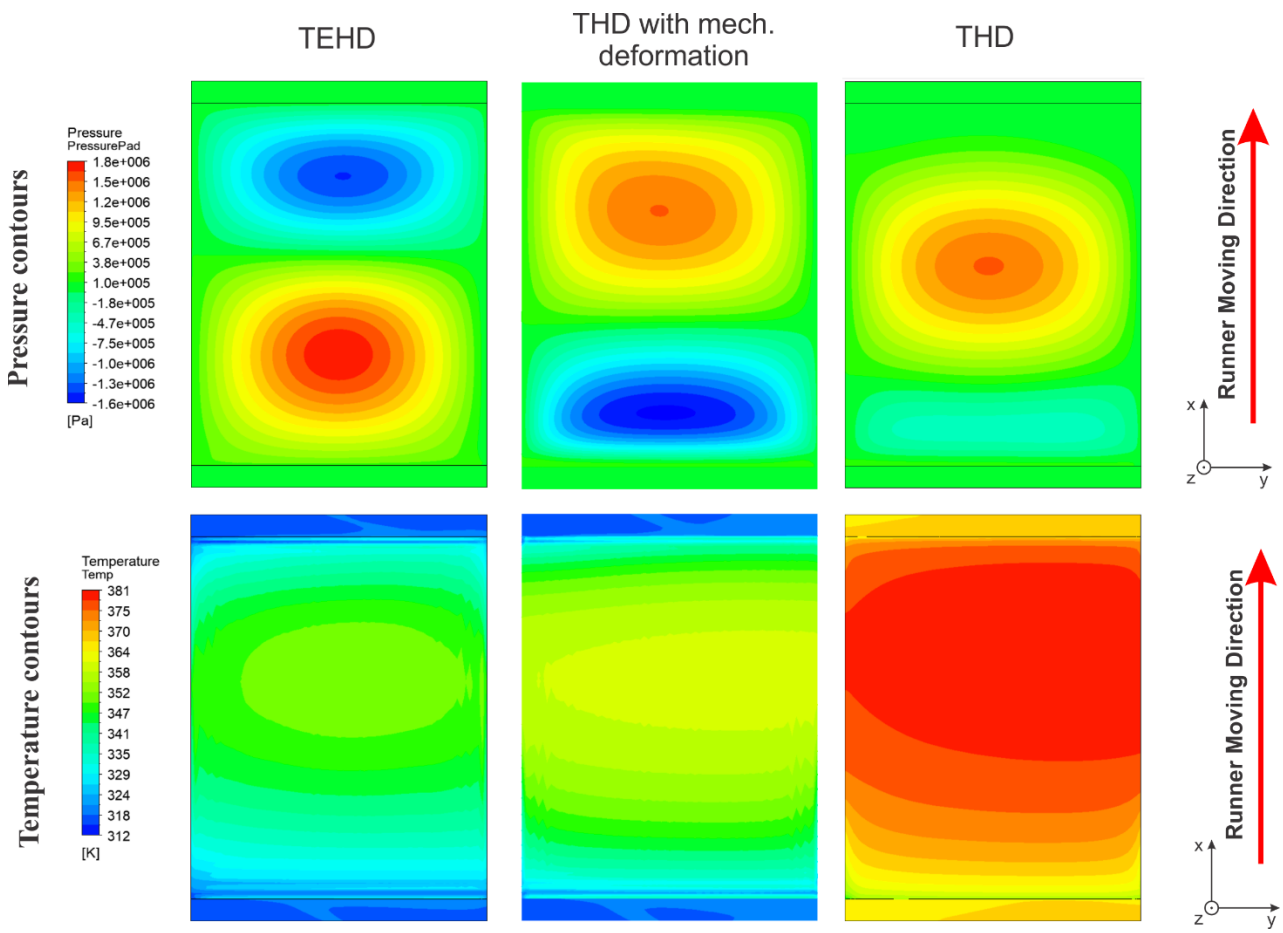

Fig. 10 – Pressure and temperature contours of the fluid/pad interface for constant load for the three different models

Effect of Initial Defect Amplitude on Bearing Performance

A parametric study has been performed on the upper pad surface to investigate how a defect, in the present case of a macroscopic sinusoidal geometry, can contribute to the supporting load of the parallel slider. In Fig. 11, the initial upper surface of the pad is depicted, for different defect amplitude values, in particular 2 μm, 1 μm, 0.5 μm, and 0.2 μm. All other bearing parameters are kept constant; runner velocity is assumed 22 m/s.

In Fig. 12, pressure, temperature, and mesh displacement profiles are presented. All the resulting fields are similar with the cases of higher defect amplitudes exhibiting higher values of pressure and decreased values of pad surface elastic deformation. In Fig. 13, the differences of the initial geometry can be observed. In the pressure profiles, as the initial defect amplitude increases the pressure positive area increases and the absolute value of the minimum pressure decreases, resulting in a higher load carrying capacity for the same H_{min}, or, equivalently, in a higher H_{min} for the same load carrying capacity. Moreover, whatever the amplitude of the defect, the positive pressure zone is always located in the first half of the pad, which is in good agreement with the pressure measured by Henry et al. [3]. Also, larger initial defect amplitude result in slightly lower temperatures. The final fluid profiles differ not only due to the initial defect amplitude, but also due to the different thermal deformation of the pad. For large amplitude defects, the thermal deformation of the bearing pad is at least three times the value of the initial defect amplitude, whereas at small defect amplitudes, this figure attains a value of 20. Therefore, for the bearing exhibiting a 2 μm defect, the final film wedge shape has a larger converging region than that of the bearings with smaller defect amplitudes, driving to the conclusion that the initial surface of macroscopic sinusoidal defect improves the

performance as the defect amplitude increases. Those results do not conclude that all initial macroscopic defects improve the behaviour of a parallel thrust slider, but there are demonstrative for a large percentage of the observed ones. Usually, the machining processes utilised in thrust slider manufacturing leads to pad profiles that resemble a sinusoidal or a convex profile, thus, the results are representative for a vast majority of the of initial surface defects present in bearing manufacturing.

The load carrying capacity of the quasi-parallel thrust slider is partially affected by the surface defect, but this is not the main pressure build-up mechanism, as it can been seen in Fig. 14. The defect amplitude of 0 μm line represents a perfect parallel thrust slider, indicating that the fact that initial surface defect just contributes to the load carrying capacity, and that the main mechanism of pressure build-up must be the thermal deformation of the pad geometry. This is also supported by the experimental study of Henry et al. [25], who have analyzed the behavior during the startup period of polished and rough pad surfaces (the later could be considered as a surface with small geometrical local defects) of two parallel surface thrust bearings. The main difference observed for the bearing with a rough surface, is the faster initiation of the hydrodynamic pressure build-up.

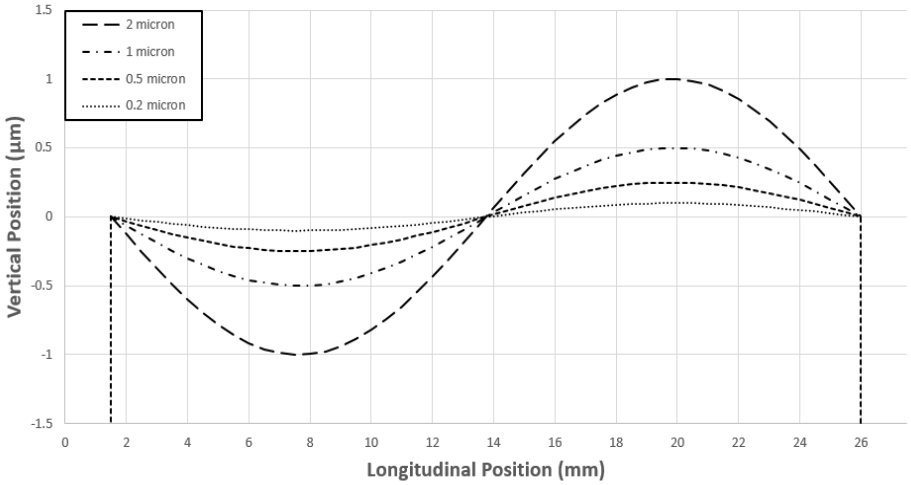

Fig. 11 - Initial pad quasi-parallel surface.

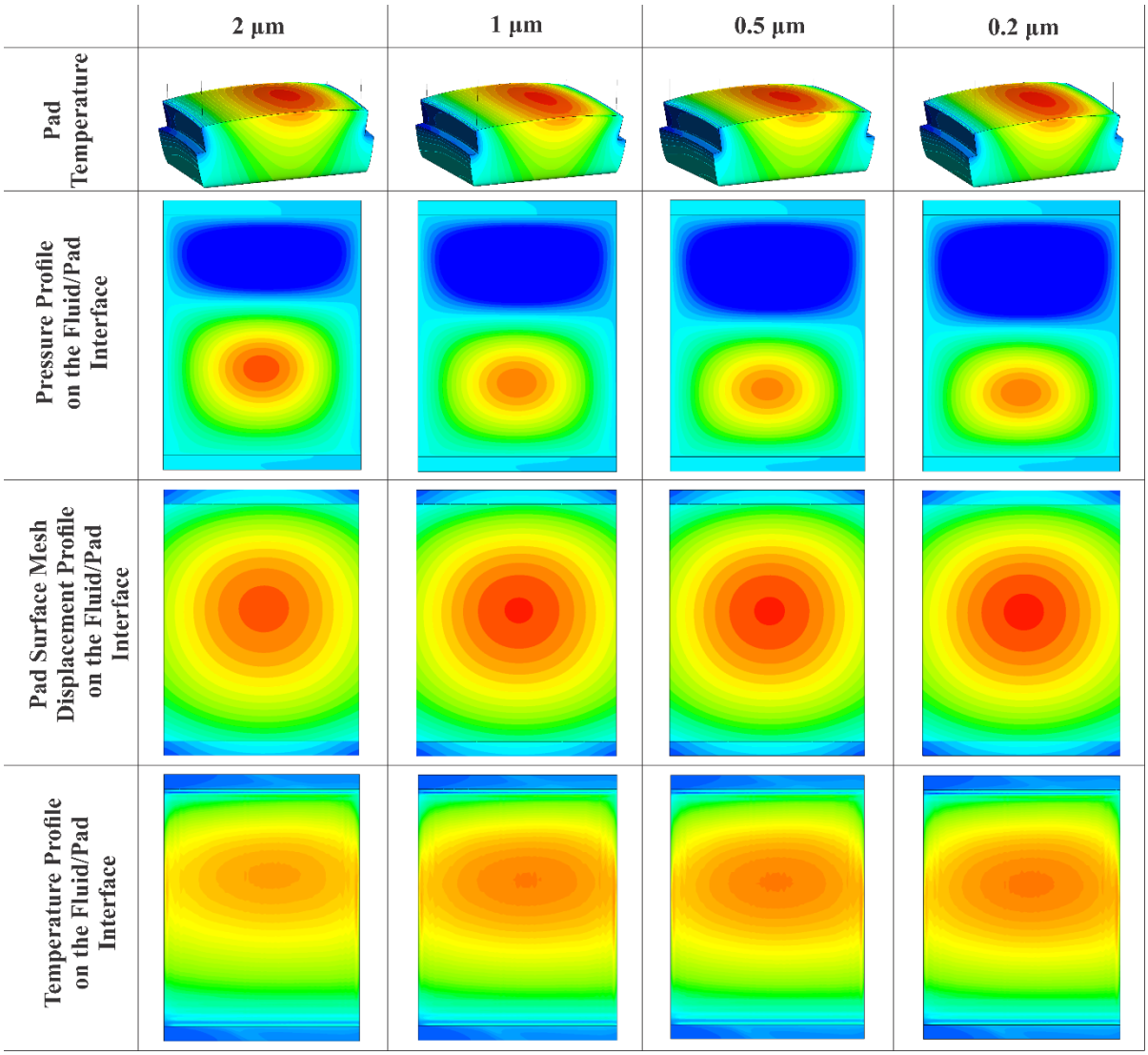

Fig. 12 – Mesh displacement, pressure and temperature profiles for different initial defect amplitudes (0.2 – 2 µm).

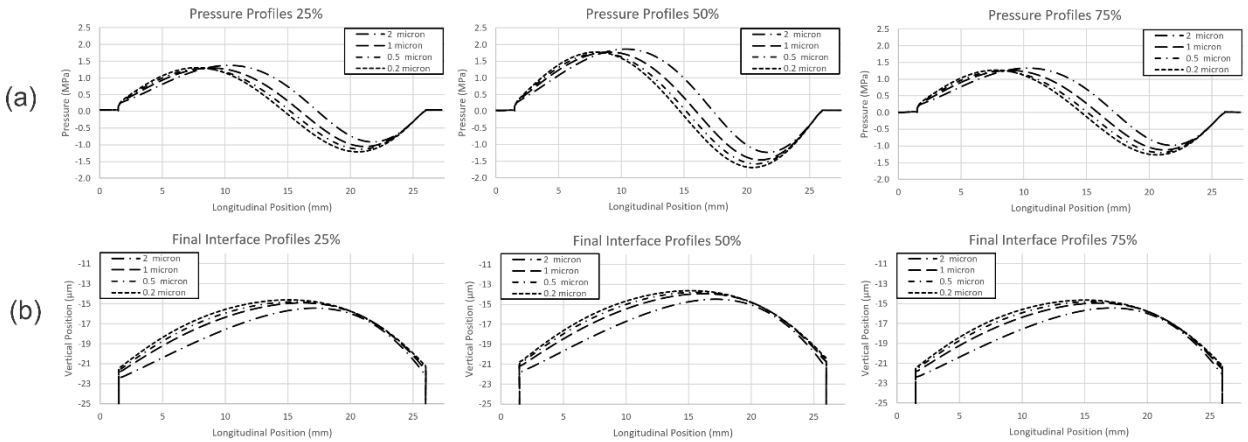

Fig. 13 – Longitudinal section profiles for varying initial defect amplitudes at the 25%, 50%, and 75% of bearing width, (a) regarding pressure, and (b) regarding the final interface profile.

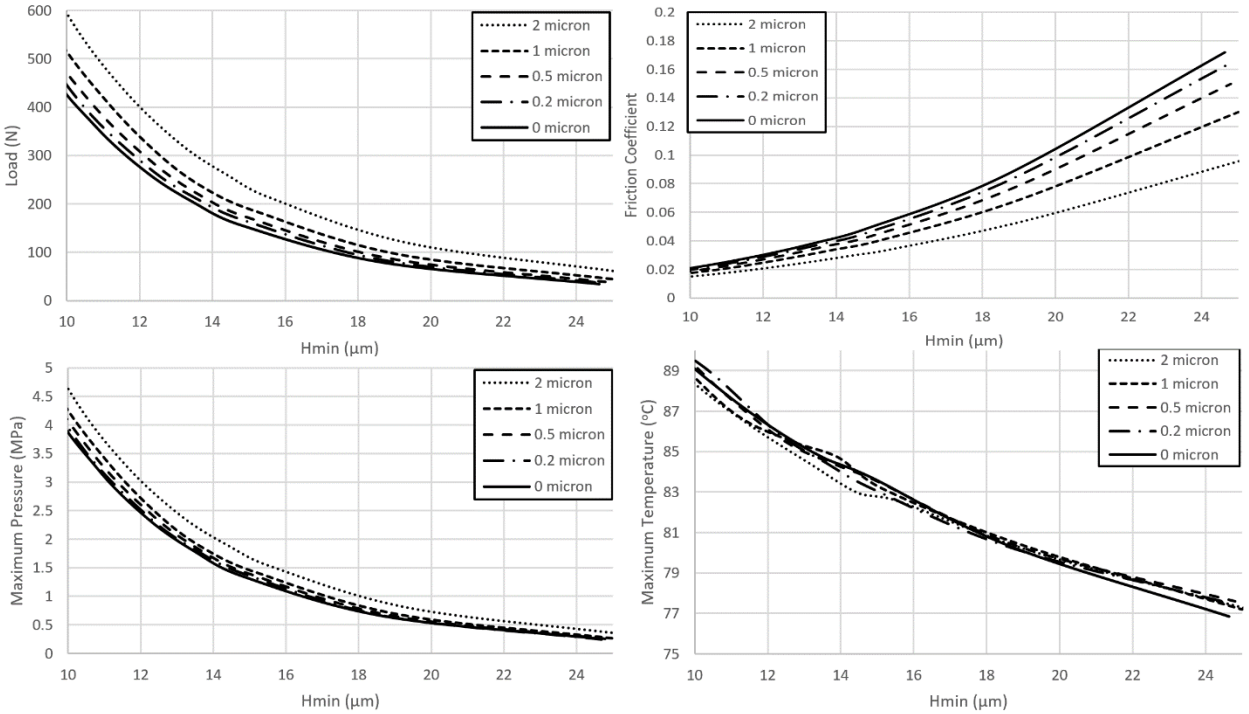

Fig. 14 – Plots of load, friction, maximum pressure, and maximum temperature versus minimum film thickness, for varying initial defect amplitude, ranging from 0 to 2μm.

Study of Bearing Performance at Different Thrust Loads

In order to explain how the thermal deformation affects the fluid film geometry, a parametric study for a constant initial geometry and velocity has been performed. The varying parameter for the current study is the load carrying capacity. The longitudinal points of maximum and minimum pressure are almost identical in all studied configurations, as it can be observed in pressure profile of Fig.15. Moreover, the final pad deformation is of the same shape, but as the load carrying capacity increases, the maximum deformation increases, but not proportionally. The resulting thermally generated fluid wedge angle increases as the load increases, producing shapes resembling more and more those of a tapered land slider bearing.

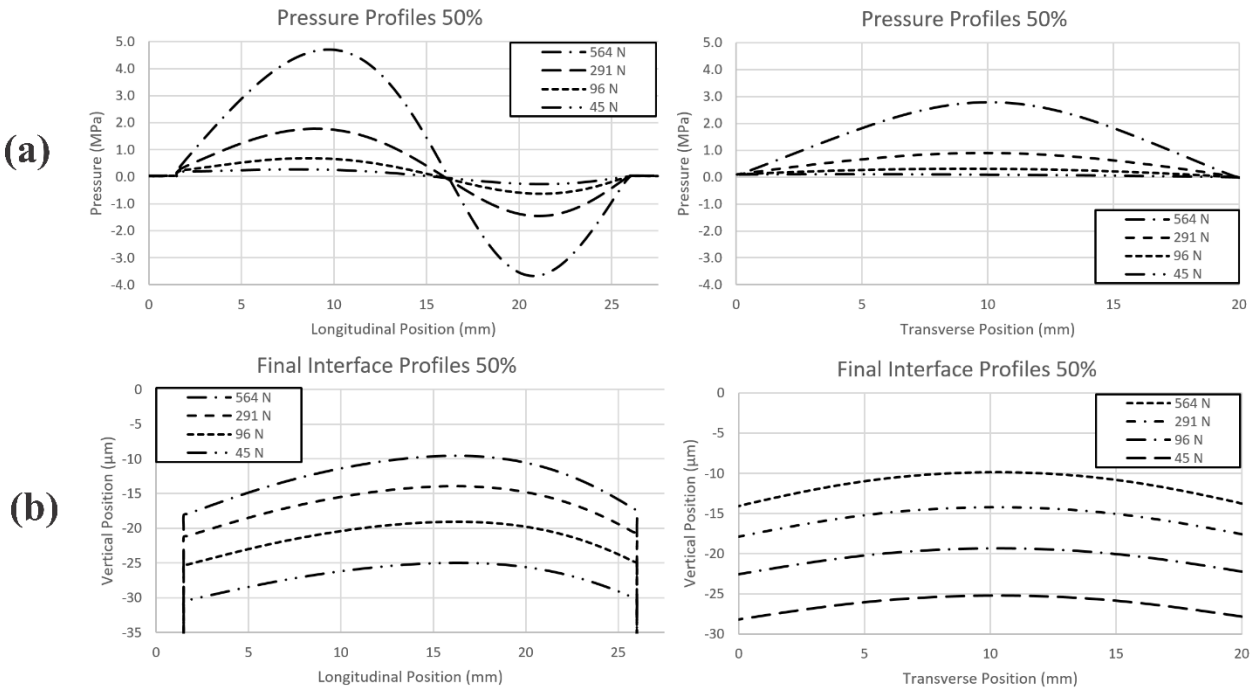

Fig. 15 – Longitudinal and transverse section profiles for varying load carrying capacity at the 50% of the width and the length, (a) regarding pressure, and (b) regarding the final interface profile.

CONCLUSIONS

In the present work, three different studies have been conducted in order to quantify the significance of different phenomena occurring in the parallel thrust slider bearings. First, three different models have been generated, namely a THD model, a TEHD model, and a THD model with mechanical deformation not including the effect of thermal deformation of the bearing pad. From the results of those three models, it can be concluded that the THD model and the THD model with mechanical deformations both underestimate the value of H_{min} for given load carrying capacity, thus resulting in a smaller maximum load carrying capacity for given values of H_{min}. As observed in experiments, parallel thrust bearings can withstand specific loads up to 1.5MPa, which cannot be computed by the THD models of the present study (either with or without mechanical deformations), since minimum film thickness is very low, leading to high temperature rise and extremely low oil viscosity, which cannot support the high specific loads that are expected. The TEHD model computes a modified lubricant geometry with more pronounced pressure build-up regions, leading to higher values of minimum film thickness and lower oil temperatures, thus being able to support higher thrust loads. Further, the maximum pressure zone calculated by the TEHD model is in accordance with the experimental observations made by Henry et al. [25].

Continuing on the parametric analysis for the sinusoidal macroscopic surface defect, the initial surface does not play a significant role in the load carrying capacity of the slider, but it helps the geometrical shape of resulting wedge generated by the thermal deformation on the pad. As the defect amplitude increases, the load carrying capacity increases. The sinusoidal defect moves the H_{min} longitudinal position closer to the trailing edge, therefore, giving a larger converging region and a smaller diverging. The macroscopic defect studied here is not the only observed defect in the manufacturing of such sliders, but it represents a large part of them. Different macroscopics

defect shapes need to be analysed in order to be able to caracterise better the manufacturing tolerances for the thrust slider bearings.

As it can be concluded from the results, the main reason for load carrying capacity for thrust slider bearing is the thermal deformation of the fluid/pad interface, but initial surface defects and the viscosity wedge can contribute substantially to the overall performance of the slider bearing.

In order to be able to acquire better results, and more relatable with the experiments conducted in other works, the presented models need to take into account cavitation. Further, the present results demonstrate that introduction of initial defects on the bearing surface may affect substantially bearing performance, especially at high values of defect amplitude. Therefore, for the characterization of the tolerances of quasi-parallel thrust slider bearings, additional types of initial defects, such as convex, concave, diverging and converging shapes, at different amplitudes, need also to be studied.

REFERENCES

[1] A. Fogg, 1946, “Fluid Film Lubrication of Parallel Thrust Surfaces”, Proceedings of the Institution of Mechanical Engineers, Vol 155, Issue 1, pp. 49 - 67.

[2] C. L. Robinson, A. Cameron, 1975, “Studies in Hydrodynamic Thrust Bearings. The parallel surfaced bearing”, Philosophical Transactions of the Royal Society of London. Series A, Mathematical and Physical Sciences, Vol. III 278, pp. 386-395.

[3] Henry Y., Bouyer J., Fillon M., 2014, “An experimental analysis of the hydrodynamic contribution of textured thrust bearings during steady-state operation: A comparison with the untextured parallel surface configuration”, Journal of Engineering Tribology, Vol 229, pp 362-375.

[4] S. Taniguchi, C. Ettles, 1975, “A Thermo-Elastic Analysis of the Parallel Surface Thrust Washer”, ASLE transactions, Vol 18, Issue 4, pp 299-305.

[5] R. A. Burton, 1963, “Effects of Two-Dimensional, Sinusoidal Roughness on the Load Support Characteristics of a Lubricant Film”, J. Basic Eng., Vol. 85, Issue 2, pp. 258-262.

[6] D. B. Hamilton,, J. A. Walowit, C. M. Allen, 1966, “A Theory of Lubrication by Microirregularities”, J. Basic Eng., Vol. 88, Issue 1, pp. 177-185.

[7] A. O. Lebeck, 1987,”Parallel Sliding Load Support in the Mixed Friction Regime. Part 2—Evaluation of the Mechanisms”, J. Tribol., Vol. 109, Issue 1, pp. 196-205.

[8] J. N. Anno, J. A. Walowit, C. M. Allen, 1968, ”Microasperity Lubrication”, J. of Lubrication Tech., Vol. 90, Issue 2, pp. 351-355.

[9] M. E. Salama, 1950, “The Effect of Macro-Roughness on the Performance of Parallel Thrust Bearings”, Proceedings of the Institution of Mechanical Engineers, Vol 163, Issue 1, pp. 149-161.

[10] D.J.Hargreaves, 1991, “Surface waviness effects on the load-carrying capacity of rectangular slider bearings”, Wear, Volume 145, Issue 1, pp. 137-151.

[11] A.G. Charitopoulos, E.E. Efstathiou, C.I. Papadopoulos, P.G. Nikolakopoulos, L. Kaiktsis, 2013, “Effects of manufacturing errors on tribological characteristics of 3-D textured”, CIRP Journal of Manufacturing Science and Technology, Vol.6, pp. 128–142.

[12] C. M. M. Ettles, A. Cameron, 1965, “The Action of the Parallel-Surface Thrust Bearing”,Proceedings of the Institution of Mechanical Engineers, Conference Proceedings, Vol 180, Issue 11, pp. 61 - 75.

[13] I. G. Currie, C. A. Brockley, F. A. Dvorak, 1965, “Thermal Wedge Lubrication of Parallel Surface Thrust Bearings”, J. Basic Eng., Vol.87, Issue 4, pp. 823-830.

[14] A. Cameron, 1958, “The Viscosity Wedge”, ASLE Transactions,Vol. 1, Issue 2, pp. 248-253.

[15] A. K. Tieu, 1975, “A Numerical Simulation of Finite-Width Thrust Bearings, Taking into Account Viscosity Variation with Temperature and Pressure”, Journal of Mechanical Engineering Science, Vol 17, Issue 1, pp. 1-10.

[16] Tan Wan Kim, Yong Joo Cho, 2008, “The Flow Factors Considering the Elastic Deformation for the Rough Surface with a Non-Gaussian Height Distribution”, Tribology Transactions,Volume 51, Issue 2, pp. 213-220.
[17] E. J. Hahn and C. F. Kettleborough, 1968, “The Effects of Thermal Expansion in Infinitely Wide Slider Bearings—Free Thermal Expansion”, J. of Lubrication Tech., Vol. 90, Issue 1, pp. 233-239.
[18] G. Xu, 1998, “A Thermal Elastohydrodynamic Lubricated Thrust Bearing Contact Model”, International Compressor Engineering Conference, Paper 1226.
[19] Liming Zhai, Yongyao Luo, Zhengwei Wang, Xin Liu, 2015, “3D Two-way Coupled TEHD Analysis on the Lubricating Characteristics of Thrust Bearings in Pump-turbine Units by Combining CFD and FEA”, Chinese Journal of Mechanical Engineering, Vol. 29, Issue 1, pp. 112–123.
[20] P. Huang, C. M. Rodkiewicz, 1999, “Thrust Bearings In the 2-D Thermal Elastohydrodynamic Lubrication: On the Slider Velocity Corresponding to the Maximum Load”, Tribology Transactions,Vol. 42, Issue 3, pp. 523-528.
[21] J. A. Greenwood, J. J. Wu, 1995, “Elasto-hydrodynamic lubrication of centrally pivoted thrust bearings”Journal of Physics D: Applied Physics, Vol. 28, No 2371.
[22] Chung-Moon Chen, D. W. Dareing, 1976, “The Contribution of Fluid Film Inertia to the Thermohydrodynamic Lubrication of Sector-Pad Thrust Bearings”, J. of Lubrication Tech, Vol. 98, Issue 1, pp. 125-132.
[23] C. I. Papadopoulos, L. Kaiktsis, M. Fillon, 2013, “Computational Fluid Dynamics Thermohydrodynamic Analysis of Three-Dimensional Sector-Pad Thrust Bearings With Rectangular Dimples”, Journal of Tribology, Vol. 136, Issue 1, No 011702.
[24] J. Frene, D. Nicolas, B. Degueurce, D. Berthe, M. Godet, 1997, “Hydrodynamic lubrication: Bearings and thrust bearings.”, Elsevier, Vol. 33.
[25] Henry Y., Bouyer J., Fillon M., 2018, “Experimental analysis of the hydrodynamic effect during start-up of fixed geometry thrust bearings”, Tribology International, Vol 120, pp 299-308.

NOMENCLATURE

H_{min}:	Minimum film thickness (μm)
V:	velocity vector (m/s)
p:	the static pressure (Pa)
T:	the temperature (K)
τ:	the viscous stress tensor
ρ:	the oil density (kg/m^3)
μ:	the oil dynamic viscosity (kg/(m*s))
c_p:	oil specific heat capacity (J/(kg*K))
λ_f:	oil thermal conductivity (W/(m*K))
λ_{sp}:	pad thermal conductivity (W/(m*K))
λ_{sr}:	slider thermal conductivity (W/(m*K))
[D]:	elasticity matrix
$\{\varepsilon^{el}\}$:	elastic strain vector
$\{\varepsilon\}$:	total strain vector
$\{\varepsilon^{th}\}$:	thermal strain vector
α^{se}:	secant coefficient of thermal expansion

APPENDIX

MESH STUDY

Two seperate mesh studies have been conducted (a) for varying number of elements in the longitudinal direction, and (b) for varying the element number in the cross-flow direction (film thickness). In all presented cases, the number of elements in the transverse direction is the half of the elements in the longitudinal direction.

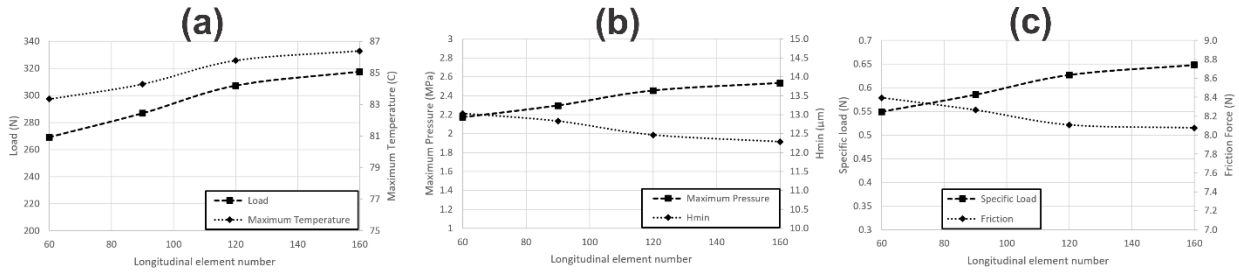

Fig. A.1 - Calculated values of (a) load carrying capacity and maximum temperature, (b) Maximum pressure and minimum film thickness, and (c) Specific load and friction force, for varying number of elements in the longitudinal direction.

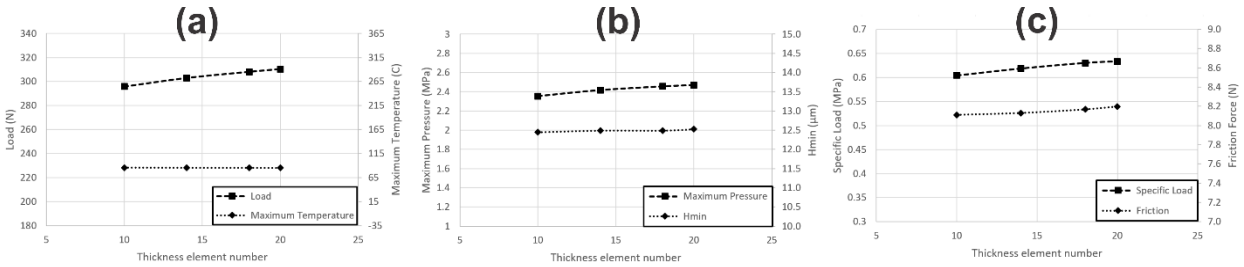

Fig. A.2- Calculated values of (a) load carrying capacity and maximum temperature, (b) Maximum pressure and minimum film thickness, and (c) Specific load and friction force, for varying number of elements in the cross-flow direction (across the fluid thickness).

Taking into consideration Fig. A.1 and Fig. A.2, the number of elements selected for the longitudinal direction was 120, and for the fluid thickness direction 18. Comparing the results of the models with those values, with the models with the higher number of elements, the accuracy is very good in terms of the goals of the present study.

CONVERGENCE STUDY

In order to calculate the TEHD model, an iterative procedure is needed, alternating the calculations between the FE and the CFD solvers. The amount of iterations needed to fully converge to the solution was not known. In order to investigate the required number of iterations needed, a convergence study has been conducted.

Regarding the maximum number of iterations, Fig. A.3 presents calculations of the main bearing performance indices, namely thrust load, maximum lubricant temperature, maximum lubricant pressure, minimum film thickness, specific load and friction force, as a function of iteration number. Based on the results, an iteration number value of 25 has been selected. This value yields a relative error of 2.7%, 0.037%, 2.9%, 0.8%, 2.7% and 0.22% of the six performance indices of the bearing, in comparison to the values corresponding to iteration number 52 (fully converged model). Calculation up to an iteration number of 52 leads to extreme computational times (25 iterations: required time is 3 days and 10 hours in 24 CPUs, 52 iterations: required time is approximately 6 days). In all cases, the maximum value of mesh displacement between two consecutive steps, after the 25th iteration was always less than 3e10-8, well below the minimum defect amplitude.

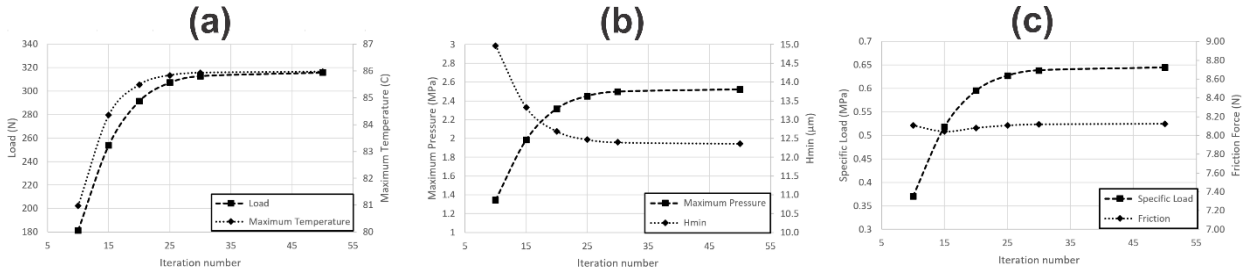

Fig. A.3 - (a) Calculated load carrying capacity and Max. temperature, (b) Max. pressure and H_{min}, and (c) Specific load and friction Force, for varying number FE-CFD iterations.